Catalysis Communications 43 (2014) 102–106

Contents lists available at ScienceDirect

Catalysis Communications

journal homepage: www.elsevier.com/locate/catcom

Short Communication

Promotion of Sn on the Pd/AC catalyst for the selective hydrogenation of cinnamaldehyde

Jia Zhao, Xiaoliang Xu, Xiaonian Li *, Jianguo Wang **

Industrial Catalysis Institute of Zhejiang University of Technology, State Key Laboratory Breeding Base of Green Chemistry-Synthesis Technology, Hangzhou, 310014, PR China

ARTICLE INFO

Article history:
Received 3 July 2013
Received in revised form 11 September 2013
Accepted 19 September 2013
Available online 26 September 2013

Keywords:
Sn-modified
Pd–Sn alloy
Cinnamaldehyde
Selective hydrogenation

ABSTRACT

The effect of Sn on the Pd/AC catalysts for the selective hydrogenation of cinnamaldehyde (CALD) was investigated. TEM, EDX, XRD and XPS have been employed to characterize Pd–Sn/AC. 80% cinnamyl alcohol (COL) selectivity can be obtained at 96% CALD conversion, even 100% selectivity can be achieved at 3% conversion. The PdSn type alloy is responsible for the enhancement of unsaturated alcohol (UA) selectivity, as confirmed by XRD and EDX. XPS technique confirmed that the promoting effect of Sn was related to Pd–Sn interaction. The favorable adsorption of C = O bond on the PdSn has been supported by means of density functional theory.

1. Introduction

Cinnamyl alcohol (COL) as a representative unsaturated alcohol (UA) is widely used in perfumery and as a deodorant [1]. In addition, the hydrogenation of cinnamaldehyde (CALD) is a suitable model reaction to investigate the effect of catalyst structure on selectivity. The hydrogenation of CALD can occur at either olefinic or carbonyl groups. The former leads to the formation of hydrocinnamaldehyde (HCAL), and the latter results in COL. Further hydrogenation can obtain hydrocinnamyl alcohol (HCOL). Forming HCAL is also thermodynamically preferred and can be achieved easily compared to forming COL.

The UA is the desired product, but over most nonpromoted monometallic catalyst the saturated aldehyde is selectively formed [2]. Great efforts have been made to improve the UA selectivity, such as alloying with a second metal. Recently, the tin alloying of Ru has been extensively applied in the selective hydrogenation of carbonyl group. For instance, Galvagno [3] reported that Ru–Sn/AC catalyst exhibited 80% selectivity to UA not above 30% conversion. Moreover, when Ru–Sn catalysts are supported on reducible oxides such as TiO_2, even 87.8% UA selectivity can be obtained at 21% citral conversion [4]. However, it was observed that UA selectivity would be decreased with the increase of conversion. Therefore, to find a stable catalyst with high selectivity and good conversion has become an increasingly urgent issue. Based on that, more and more attention has been attracted on Pd–Sn alloy catalysts as potential catalysts in selective unsaturated aldehydes hydrogenation reactions. Mahmoud [5] studied the influence of additives such as Ir, Cu, and Sn on Pd/SiO_2 catalysts for CALD hydrogenation. They did not observe a decrease in HCAL selectivity upon Ir or Cu addition onto Pd. However, a decrease in the HCAL selectivity was observed after Sn addition onto Pd, which can be attributed to the formation of a Pd_2Sn structural phase. Better catalytic performance of Pd–Sn bimetallic catalysts was obtained by Vicente [6] who reported that higher than 75% UA selectivity could be reached at 30% citral conversion when Pd_3Sn was formed in $Pd–Sn/SiO_2$ catalysts. The influence of tin on the catalytic selectivity of Pd/AC, for one thing, can be attributed to the interaction between oxidized tin species and the oxygen atom of the carbonyl bond, thus weakening the C = O bond and favoring its hydrogenation. For another, the dilution effect of Pd caused by Sn can significantly enhance the selectivity of UA intermediates through the conversion of the on-top adsorption mode of the carbonyl group.

Despite the effectiveness of Pd–Sn alloy phases such as Pd_3Sn and Pd_2Sn being employed to catalyze selective hydrogenation of unsaturated aldehydes, the problem of lack of stability of UA selectivity particularly at high conversion was still not resolved. With the aim of improving the yield toward the hydrogenation of the carbonyl bond, an unreported Pd–Sn/AC catalyst bearing PdSn structure alloy was prepared and analyzed. The excellent performances of Pd–Sn/AC in the hydrogenation of CALD into COL were obtained.

2. Experimental section

2.1. Catalyst preparation and characterization

A commercially starting activated carbon with particle size less than 61 μm, specific surface area of 1703 m^2/g was made from coconut shells (Fujian Xinsen Carbon Co., Ltd. China). The Sn-modified Pd/AC catalysts

* Corresponding author. Tel.: +86 571 88320002.
** Corresponding author. Tel.: +86 571 88871037.
E-mail addresses: xnli@zjut.edu.cn (X. Li), jgw@zjut.edu.cn (J. Wang).

1566-7367/$ – see front matter © 2013 Elsevier B.V. All rights reserved.
http://dx.doi.org/10.1016/j.catcom.2013.09.019

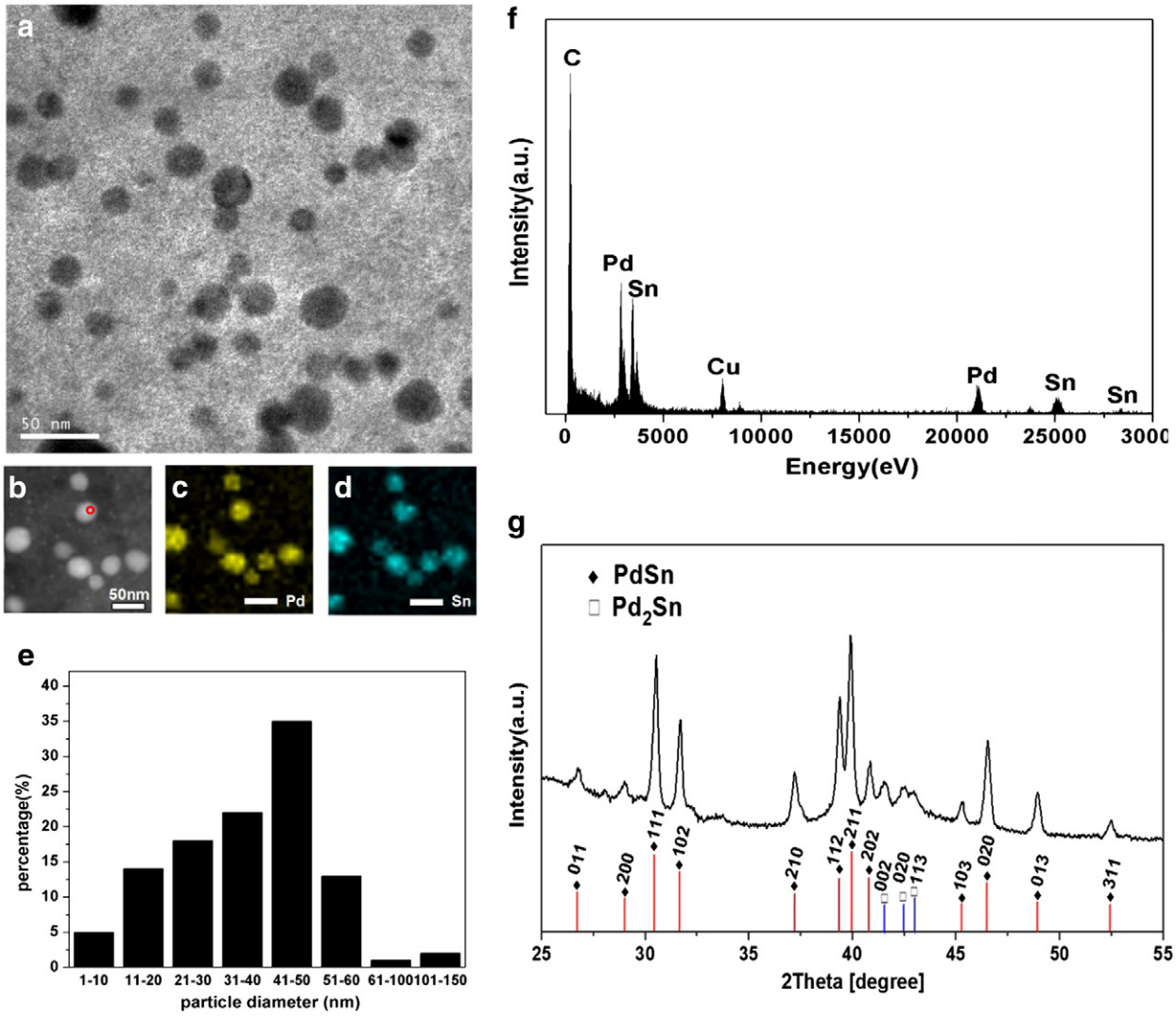

Fig. 1. Characterization of the prepared Pd–Sn NPs:(a) TEM image, (b–d) HAADF-STEM images together with the EDX mapping, (e) histograms of the particle size, (f) point-scanning spectrum of an individual Pd–Sn NP, and (g) XRD pattern.

were prepared by incipient wetness impregnation with precursors of $SnCl_2{\cdot}2H_2O$ and aqueous solution of H_2PdCl_4 (0.05 g_{metal}/mL). After $SnCl_2{\cdot}2H_2O$ was charged into an aqueous slurry of the carbon support (the ratio of support to water was 1 g:10 mL), H_2PdCl_4 was injected into the above solution at 353 K. Then the pH value 8–9 was adjusted using NaOH aqueous solution (10 wt.%). Subsequently, it was filtered, washed by distilled water until pH value dropped to 7, dried under vacuum at 383 K for 4 h and then calcined in N_2 gas stream at 723 K for 4 h. The obtained products were dissolved in deionized water and $SnCl_2{\cdot}2H_2O$ was once again charged into aqueous slurry of the obtained samples under mild stirring. After impregnation, the samples were treated according to the aforementioned procedure, except that the samples were calcined at 823 K. Finally, the samples were reduced in H_2 stream at flow rate of 20 mL/min at 773 K. The actual contents of Pd and Sn of Pd–Sn/AC were determined by XRF analysis acquired with a Thermo ARLADVANT'X IntelliPower TM 4200 spectrometer, their contents are 2.01% and 3.32% respectively. For comparison, Pd/AC and Sn/AC were prepared using the same procedures. The actual contents of Pd and Sn were 1.96% and 3.51% respectively, determined by XRF analysis. A commercial 2 wt.% Pd/C catalyst (as received from JiangXiHan's platinum industry co., LTD. China.) also was employed as a comparison.

The microstructure and components of the alloy NPs were examined by TEM equipped with high-angle annular dark-field (HAADF) attachment and EDX spectroscopy (Philips-FEI Tecnai G2 F30 S-Twin). At least 500 particles for each sample were randomly measured to calculate average particle size. XRD measurements of the catalyst samples were performed on a PANalytical-X'Pert PRO generator with Cu Kα radiation ($\lambda = 0.1541$ nm). XPS was acquired with a Kratos AXIS Ultra DLD spectrometer. XPS analysis was performed with the monochromatized aluminum X-ray source and pass energy of the electron analyzer of 40 eV. The pressure in the sample analysis chamber was lower than 6×10^{-9} Torr during data acquisition. Binding energies were referred to the C1s line at 284.8 eV.

2.2. Typical procedure for the hydrogenation of CALD

The reaction mixture, composed of 0.1 g catalyst, 3.0 mL CALD, and 200 mL 95 vol% isopropanol (10 mL neat water contained), was introduced into a 500-mL autoclave. Air in the autoclave was purged by hydrogen, and then the reaction proceeded at the required temperature (403 K) and at 7 MPa of 99.99% pure hydrogen. Only CALD, HCAL, HCOL and COL are detected as the reaction products under the

experimental conditions used, which are quantified by using n-heptane as the internal standard substance, and the carbon balance values are near 100% based on these products. The conversion and selectivity were calculated with the formulas:

$$Conversion_{CALD} = \left(1 - \frac{m_{CALD}\%}{m_{CALD}\% + m_{HCAL}\% + m_{COL}\% + m_{HCOL}\%}\right) \times 100\%$$

$$Selectivity_{COL} = \frac{m_{COL}\%}{m_{COL}\% + m_{HCAL}\% + m_{HCOL}\%} \times 100\%$$

2.3. DFT calculation

All the density functional theory (DFT) calculations were implemented with the $DMol_3$ module in Material Studio [7]. The generalized gradient approximation with Perdew-Wang (PW91) [8] was used to describe the exchange-correlation effects. The double numerical basis sets augmented with polarization functional, which has a computational precision being comparable with split-valence basis set 6-31 g**, were applied in the expanded electronic wave function, where effective core potentials were used to describe Pd and Sn atoms. The Brillouin-zone integration sampling was performed with $2 \times 2 \times 1, 2 \times 2 \times 1, 3 \times 3 \times 1$ for Pd (111), PdSn (211) and Pd_3Sn (111) surfaces. In the calculations, the tolerance for self-consistent field was set to 1.0×10^{-6} eV. The adsorption of CALD molecule on the PdSn alloy catalysts is typically calculated according to the formula: Eads = E (ad) + E (sub) − E (sub + ad). Where E (ad + sub) is the total energy of CALD molecule adsorbed on the PdSn alloy catalysts and both E (sub) and E (ad) are the total energies of the PdSn alloy catalysts and CALD molecule, respectively.

Table 1
Catalytic results of the hydrogenation of CALD [a].

Catalyst	Reaction rate (mol g_{Pd}^{-1} h^{-1}) [b]	Sel. (%) [c]		
		HCAL	COL	HCOL
Commercial Pd/C	1.53	85.98	2.49	11.53
Pd/AC	0.67	81.96	12.82	5.22
Pd–Sn/AC	0.39	2.82	88.04	9.14
Sn/AC	/	/	/	/

[a] Reaction conditions: 3.0 mL CALD, 0.1 g catalyst, 200 mL 95 vol% isopropanol as solvent, 403 K, 7 MPa P_{H2}.
[b] Reaction rate estimated between 0% and 10% CALD conversion.
[c] Selectivity estimated at 50% CALD conversion.

3. Results and discussion

Fig. 1a showed that Pd–Sn particles are of spherical-like shape and uniformly dispersed on the AC support. Their sizes of Pd–Sn particles are distributed mainly from 11 nm to 60 nm, and the mean particle size is about 40 nm (Fig. 1e). This is a consequence of a progressive broadening particle size distribution as tin is added. In the XRD patterns of Fig. 1g, the obvious crystal planes of the PdSn type alloy were observed. Typically, a slight shift in 2θ value for (211) crystallite plane of Pd–Sn (2θ = 40.128°) was observed, while the (111) crystallite plane of Pd appeared at the Bragg angle of 40.2°. This slight shift with respect to (111) crystallite plane of Pd may be probably attributed to the formation of Pd–Sn alloy. A small amount of other Pd–Sn type alloy such as Pd_2Sn also can be observed. Less metallic palladium with clear characteristic diffraction peaks can be observed, indicating that almost all the Pd phases contain some dissolved Sn. To further investigate the structure of Pd–Sn NPs, the elemental distributions of Pd and Sn were studied by a HAADF-STEM. The representative STEM image within a randomly selected area and its corresponding Pd and Sn elemental maps are shown in Fig. 1b–d. It could be seen that both Pd and Sn were evenly distributed in each individual NP. The PdSn type alloy formation between Pd and Sn is also confirmed by energy dispersive spectroscopy (EDX) point-scanning profile (Fig. 1f) across a randomly selected single particle (see red circle in Fig. 1b), which its reflection appeared that atom ratio of Pd/Sn is 0.97, as already suggested from the XRD study.

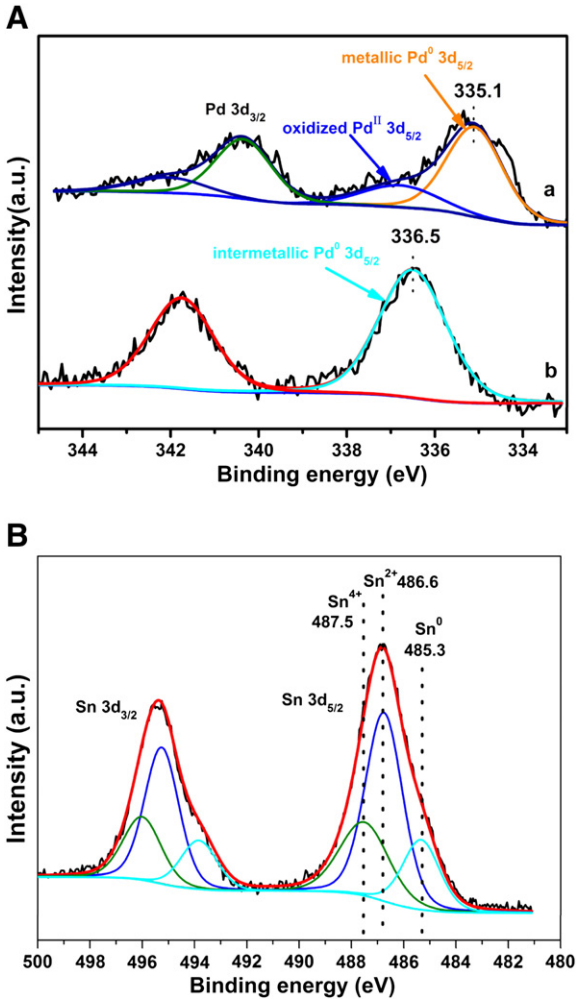

Fig. 2. (A) Pd 3d photoemission core-level spectra for Pd/AC (a) and Pd–Sn/AC (b) catalysts, (B) Sn 3d photoemission core-level spectra for Pd–Sn/AC.

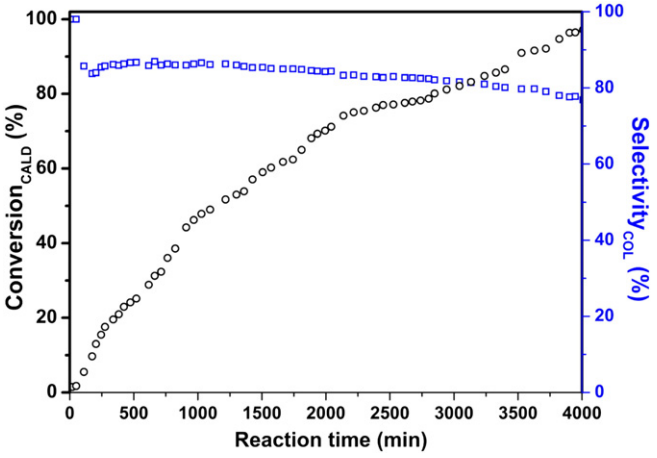

Fig. 3. Conversion and UA selectivity of CALD as a function of reaction time (min) for 0.1 g of Pd–Sn/AC catalyst at 403 K and 7 MPa H_2 pressure (□ COL selectivity, ○ conversion).

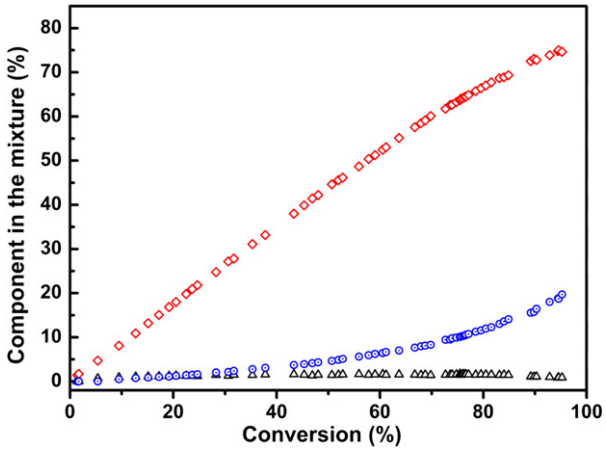

Fig. 4. Conversion of 1.5% (v/v) CALD/solvent over 0.1 g of Pd–Sn/AC catalyst at 403 K and 7 MPa H_2 pressure (△ HCAL, ⊙ HCOL, COL).

To further understand the interactions among Pd and Sn, the surface properties and the chemical states of Pd and Sn were investigated by XPS. Fig. 2A shows the XPS spectra of Pd 3d core level of Pd/AC and Pd–Sn/AC catalysts. Pd/AC catalyst presented two peaks of Pd $3d_{5/2}$ core level at the binding energy (BE) of 335.1 eV and 336.8 eV, respectively. For the Pd–Sn/AC catalyst, the peak related to Pd species appeared at 336.5 eV corresponding to the Pd $3d_{5/2}$ core level. As is established in the literature, the binding energy of metal state Pd^0 is at about 335.0–335.1 eV, the oxidized Pd ($Pd^{II}O$) is at about 336.6–336.8 eV, and while the Pd–Sn intermetallic state Pd is about 336.3–336.4 eV [9]. These showed that Pd–Sn intermetallic compounds are formed and that all the Pd atoms are involved in the alloy formation, which strongly implies the electron transfer from Pd to Sn [10]. Vertical lines indicate the metallic tin, Sn^{2+} existing as Pd–Sn–O and/or Sn–O phases, and Sn^{4+} peak positions at about 485.3, 486.6 and 487.5 eV (left to right) for Sn $3d_{5/2}$ core levels, respectively (Fig. 2(B)) [11]. This may demonstrate that bulk of tin is still in oxidized state while the surface structure is zero-valent metal species.

The hydrogenation of CALD over each catalyst was shown in Table 1. Over the Pd/AC, which was one of the conventional hydrogenation catalysts, HCAL was given as a main product, and the selectivity of COL was 12.82%. Moreover, the selectivity of COL was only 2.49% over commercial Pd/C catalyst. A higher activity of commercial Pd/C catalyst compared with Pd/AC catalyst was attributed to a sintering effect of the active metal phase after a calcined treatment at 823 K for the Pd/AC catalyst. Addition of Sn to Pd/AC brought about the increasing selectivity of COL up to 88.04%. This result agreed with the previous reports, which indicated that the addition of Sn led to the acceleration of the activation of C = O group [12]. A higher addition of tin reduces the initial hydrogenation rate, which may be due to the lowered number of active sites. As for Sn/AC, the hydrogenation reaction did not proceed because of the absence of the site activating hydrogen.

The catalytic performances of Pd–Sn/AC in the hydrogenation of CALD into COL were shown in Fig. 3. The experimental results indicated that a high selectivity could be reached, even at high conversion of CALD. Moreover, the results as in Fig. 4 showed that the hydrogenation of CALD to HCAL might be suppressed extremely. 80% selectivity towards the corresponding COL can be obtained at 96% CALD conversion, and even 100% selectivity might be obtained at 3% CALD conversion with the Pd–Sn/AC.

The geometric and electronic modifications of Pd caused by Sn may be used to explain the observed results. It has been suggested that on the larger particles the aromatic ring lies at a distance exceeding 0.3 nm due to the presence of an energy barrier which prevents a closer approach [13–15]. Under these conditions the CALD molecule is tilted and the carbonyl group is closer to the surface of the metal. Therefore, it is believed that the carbonyl group on flat planes is easy to be activated. Therefore, the high selectivity of PdSn composition catalyst may be related to the larger metal particles partly. In addition, this promoting effect is related to the electronic modifications of Pd by Sn. The obtained allowance for initial and final state effects in the photoemission data indicated the electron transfer from Sn to Pd. It confirmed the significant Pd surface core-level shift enhancement by Sn. And the upward shift of Pd binding energy may be associated with the formation of Pd–Sn alloy, which is proposed to be responsible for the enhanced adsorption of C = O bond on the surface of Pd–Sn/AC. Maximum COL selectivity

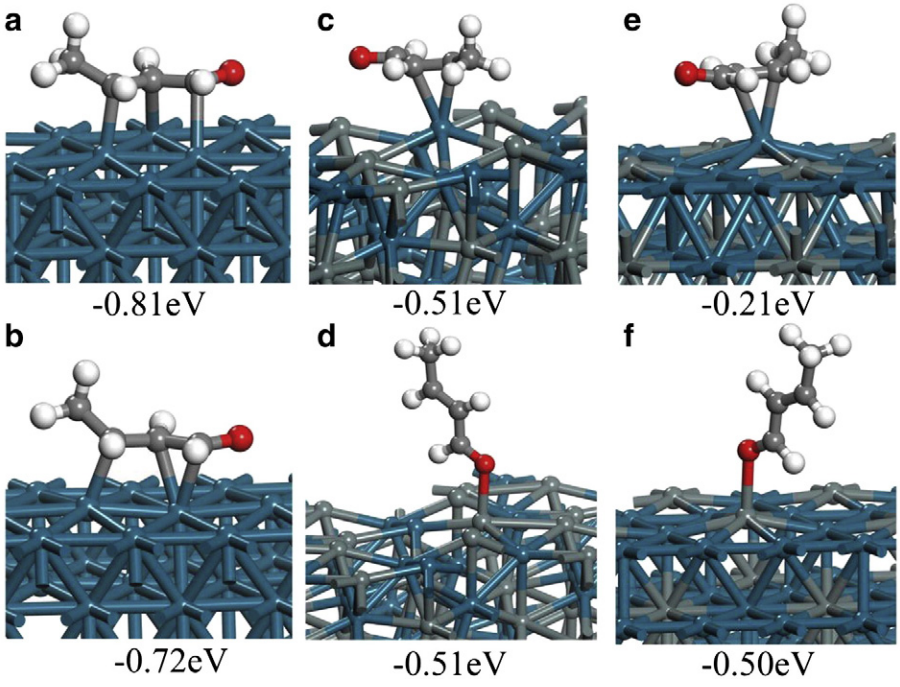

Fig. 5. The adsorption configuration and energy of crotonaldehyde on Pd (111) (a.b.), PdSn (211) (c.d.), Pd_3Sn (111) (e.f.).

was obtained when the PdSn type alloy was formed in the bimetallic particles.

In order to understand the cause of the enhanced selectivity of UA on Pd–Sn alloy catalyst, the adsorption of unsaturated aldehydes on Pd (111), Pd_3Sn (111) and PdSn (211) was calculated with the DFT calculations. As a representative of unsaturated aldehydes, crotonaldehyde was selected to investigate its adsorption of on Pd (111), PdSn (211) and Pd_3Sn (111) surfaces in this study. Fig. 5 shows the most stable structures of crotonaldehyde on these surfaces, in which crotonaldehyde is adsorbed in either C = C or C = O bonding with metals. On Pd (111) surface, the stable structure in C = O bonding with metal was not found. It is seen that the dominant adsorption mode of crotonaldehyde is the C = C bonds with Pd [16], which is responsible for the predominant product of hydrogenation of C = C bonds of unsaturated aldehydes. With the formation of alloy, the adsorption way dramatically changed. On Pd_3Sn (111), the adsorption energy of crotonaldehyde is the same in either C = C or C = O bonding with metal, which indicates that possibility of hydrogenation of C = C bonds of unsaturated aldehydes is increased. Especially on PdSn (211), the adsorption strength of crotonaldehyde is much stronger in C = O bond than that in C = C with metal surfaces. Therefore, the adsorption modes change of unsaturated aldehydes on Pd surfaces induced by Sn could be the main reason for the enhanced selectivity of unsaturated aldehyde to corresponding UA.

4. Conclusions

In conclusion, this work focused on the study of interaction between Pd and Sn in Pd–Sn/AC bimetallic catalysts for the selective hydrogenation of CALD to COL. A significant improvement to the selectivity for COL could be reached when Pd/AC catalysts was modified by Sn. The Pd–Sn bimetallic interactions in form of PdSn type alloy modify the Pd sites both geometrically and electronically and result in the significant suppressing adsorption of C = C bond. In addition, it provides new sites to activate C = O bond of CALD. The favorable adsorption of C = O bond on the uniform PdSn type alloy and C = C bonding on the Pd surfaces have been supported by means of density functional theory.

References

[1] P. Gallezot, D. Richard, Catal. Rev. Sci. Eng. 40 (1998) 81–126.
[2] U.K. Singh, M.A. Vannice, J. Catal. 199 (2001) 73–84.
[3] S. Galvagno, C. Milone, A. Donato, G. Neri, R. Pietropaolo, Catal. Lett. 17 (1993) 55–61.
[4] G. Neri, A. Donato, C. Milone, L. Mercadante, A.M. Visco, J. Chem. Technol. Biotechnol. 60 (1994) 83–88.
[5] S. Mahmoud, A. Hammoudeh, S. Gharaibeh, J. Melsheimer, J. Mol. Catal. A 178 (2002) 161–167.
[6] A. Vicente, G. Lafaye, C. Especel, P. Marécot, C.T. Williams, J. Catal. 283 (2011) 133–142.
[7] B. Delley, J. Chem. Phys. 113 (2000) 7756–7764.
[8] J.P. Perdew, Y. Wang, Phys. Rev. B 45 (1992) 13244–13249.
[9] K. Kovnir, J. Osswald, M. Armbrüster, D. Teschner, G. Weinberg, U. Wild, et al., J. Catal. 264 (2009) 93–103.
[10] I.M.J. Vilella, S.R. de Miguel, O.A. Scelza, J. Mol. Catal. A 284 (2008) 161–171.
[11] E. Esmaeili, Y. Mortazavi, A.A. Khodadadi, A.M. Rashidi, M. Rashidzadeh, Appl. Surf. Sci. 263 (2012) 513–522.
[12] A.B. Merlo, B.F. Machado, V. Vetere, J.L. Faria, M.L. Casella, Appl. Catal. A 383 (2010) 43–49.
[13] J. Teddy, A. Falqui, A. Corrias, D. Carta, P. Lecante, I. Gerber, et al., J. Catal. 278 (2011) 59–70.
[14] P. Kačer, L. Červený, Appl. Catal. A 229 (2002) 193–216.
[15] C. Minot, P. Gallezot, J. Catal. 123 (1990) 341–348.
[16] F. Delbecq, P. Sautet, J. Catal. 211 (2002) 398–406.